Activation of cathepsin L contributes to the irreversible depolarization induced by oxygen and glucose deprivation in rat hippocampal CA1 neurons

Shogo Kikuta[a, b], Yoshinaka Murai[a, *], Eiichiro Tanaka[a]

[a]*Department of Physiology and* [b]*Dental and Oral Medical Center, Kurume University School of Medicine, Kurume, Japan*

*Corresponding author at: Department of Physiology, Kurume University School of Medicine, 67 Asahi-machi, Kurume 830-0011, Japan.

E-mail addresses: ymurai@med.kurume-u.ac.jp (Y. Murai),

kikuta_shougo@med.kurume-u.ac.jp (S. Kikuta)

Conflict of Interest: All authors declare no conflict of interest.

Ethical approval: All applicable international, national, and/or institutional guidelines for the care and use of animals were followed. This article does not contain any studies with human participants.

Abstract

Oxygen and glucose deprivation (OGD) elicits a rapid and irreversible depolarization with a latency of ~5 min in intracellular recordings of hippocampal CA1 neurons in rat slice preparations. In the present study, we examined the role of cathepsin L in the OGD-induced depolarization. OGD-induced depolarizations were irreversible as no recovery of membrane potential was observed. The membrane potential reached 0 mV when oxygen and glucose were reintroduced immediately after the onset of the OGD-induced rapid depolarization. The OGD-induced depolarizations became reversible when the slice preparations were pre-incubated with cathepsin L inhibitors (types I and IV at 0.3–2 nM and 0.3–30 nM, respectively). Moreover, pre-incubation with these cathepsin inhibitors prevented the morphological changes, including swelling of the cell soma and fragmentation of dendrites, observed in control neurons after OGD. These findings suggest that the activation of cathepsin L contributes to the irreversible depolarization produced by OGD.

Keywords: hippocampus; CA1 neuron; ischemia; cathepsin L

1. Introduction

Hippocampal CA1 neurons display a stereotyped response to oxygen and glucose deprivation (OGD), characterized by an initial hyperpolarization followed by a slow depolarization, which leads to a rapid depolarization after ~5 min of exposure to OGD. When oxygen and glucose are reintroduced immediately after the rapid depolarization, the membrane depolarizes further (persistent depolarization), reaching 0 mV within 5 min after the onset of the reintroduction. The membrane never recovers to the potential before exposure to OGD (irreversible depolarization). As a result, the neurons show no functional recovery [1]. An increase in the ATP-sensitive K^+ conductance is largely responsible for the initial hyperpolarization [2]. Inhibition of the Na^+/K^+-ATPase, which results in an elevation in $[K^+]_o$, and an accumulation of glutamate contribute to the slow depolarization. The non-selective increase in ion permeability elicits the rapid depolarization [1]. The persistent depolarization is a Ca^{2+}-dependent process that is mediated by the activation of ionotropic glutamate receptors and Ca^{2+}-induced Ca^{2+} release from intracellular Ca^{2+} stores [3]. Moreover, blebs appear on the cell body of CA1 pyramidal neurons 1 min after the reintroduction of oxygen

and glucose, and the cell body becomes swollen 3 min later, resulting in irreversible cell membrane dysfunction [4].

There is considerable evidence that oxygen radicals are important mediators of tissue injury in cerebral ischemia [5-10]. The excessive production of NO induced by Ca^{2+} influx through NMDA receptor channels contributes to the irreversible depolarization produced by OGD in rat CA1 pyramidal neurons [11]. Oxygen radicals produced by the metabolism of arachidonic acid by cytochrome P-450 isozymes also play a role in the irreversible depolarization induced by OGD [12]. In addition, oxygen radicals produced by COX-2 metabolism of arachidonic acid following OGD increase lysosomal membrane permeability in the rat hippocampus [13]. Indeed, NO levels and cathepsin B and L activity increase after OGD in the rat brain [14]. Therefore, the release of lysosomal enzymes might lead to neuronal death after OGD [13].

Cathepsins are a family of acid proteases, and are classified into three subfamilies according to the amino acid in the active site that confers catalytic activity; cysteine (cathepsins B, C, F, H, K, L, N, O, S, T, U, W and X), aspartate (cathepsins D and E) and serine (cathepsins A and G). Among the lysosomal cathepsins, B, L and D are abundant in neurons [15]. Although the activity of cathepsin L markedly increases soon after OGD [16], a

few studies have shown that the activity of cathepsin B increases 2 h after OGD [13, 17]. It is therefore possible that the production of oxygen radicals by the metabolism of arachidonic acid following OGD induces cathepsin L release from lysosomes, and this may lead to the irreversible depolarization. In the present study, we examined whether cathepsin L contributes to the irreversible depolarization induced by OGD.

2. Materials and methods

2.1. Ethics

All experiments were conducted in accordance with the *Guiding Principles for the Care and Use of Animals in the Field of Physiological Science*, formulated by the Physiological Society of Japan, and had the approval of the Institutional Animal Use and Care Committee at Kurume University.

2.2. Slice preparation

Wistar rats (male, 250–350 g, 8–12 wks old) were rapidly decapitated under ether anesthesia, and the forebrains were removed and placed in chilled (4–6 °C) Krebs solution aerated with 95% O_2/5% CO_2. The composition of the Krebs solution was (in mM) 117 NaCl, 3.6 KCl, 2.5 $CaCl_2$, 1.2 $MgCl_2$, 1.2 NaH_2PO_4, 25 $NaHCO_3$ and 11 glucose. The hippocampus was dissected and then sliced (thickness of 350 μm) with a Vibrating Microtome 7000smz (Campden Instruments). A slice was placed on a nylon net in a recording chamber (volume, 500 μL) and immobilized with a titanium grid placed on the upper surface of the section. The preparation was completely submerged in the superfusion solution (temperature, 36.5 ± 0.5 °C; flow rate, 4–6 mL/min).

2.3. OGD and electrophysiology

Intracellular recordings from CA1 pyramidal cells were made with glass micropipettes filled with potassium acetate (2 M). The electrode resistance was 50–90 MΩ. In conventional intracellular recordings, the apparent input resistance in CA1 neurons was monitored by passing small hyperpolarizing pulses (0.2–0.4 nA, 200 ms) through the recording electrode every 3 s.

Ischemia was induced by superfusing the slice with medium equilibrated with 95% N_2/5% CO_2 and by iso-osmotically replacing the glucose with NaCl (oxygen- and glucose-deprived medium). When switching the superfusing medium, there was a delay of 15–20 s before the new medium reached the chamber owing to the volume of the connecting tubing. As a result, the chamber was filled with the test solution ~30 s after switching the solution. We used one slice per experiment because the responses to OGD could not be reproduced.

The latency of the rapid depolarization was measured from the onset of superfusion to the onset of the rapid depolarization estimated by extrapolating the slope of the rapid depolarization to the slope of the slow depolarization [1]. The degree of recovery after the reintroduction of oxygen and glucose was evaluated as follows: no recovery, 30–60 min after reintroduction, the membrane potential rests between 0 and −19 mV; complete recovery, the membrane potential is more negative than −60 mV; partial recovery, the membrane potential repolarizes to between −20 and −59 mV [3].

2.4. Biocytin labeling

For biocytin labeling, slices were transferred to 0.1 M phosphate buffer solution with 4% paraformaldehyde buffered to pH 7.4 within 20 s of withdrawal of the recording electrode filled with potassium acetate (2 M) and biocytin (2%). After overnight fixation, the slices were washed with alcohol (80%) and subsequently with dimethylsulfoxide (DMSO). Slices were then transferred to 0.1 M phosphate-buffered saline (NaCl, 150 mM, pH 7.0) and rinsed. The slices were pretreated with Triton X-100 (0.05%) containing Tris buffer (pH 7.0), followed by overnight incubation with Extravidin-horseradish peroxidase conjugate (1:1,000 dilution). Subsequently, the slices were reacted with diaminobenzidine (0.05%) and hydrogen peroxide (0.03%). The slices were rinsed in Tris buffer and then mounted in glycerol and examined by light microscopy.

2.5. Reagents

The following reagents were used: biocytin, Extravidin-horseradish peroxidase conjugate and diaminobenzidine (Sigma Chemical); DMSO (Wako Chemicals); hydrogen peroxide (Mitsubishi Kasei); Z-Phe-Phe-CH_2F (Z-FF-FMK/cathepsin L inhibitor I), and 1-naphthalenesulfonyle-lle-Trp-CHO (cathepsin L inhibitor IV) (Calbiochem). All drugs

were dissolved in the perfusate and applied by bath application. The slices were pretreated with media containing the drug for 10 min before the ischemic exposure. For analysis of the membrane potential 30 min post-OGD, the relative recovery ratio (%Recovery) was calculated. The membrane potential 30 min post-OGD divided by the resting membrane potential yielded the %Recovery (Fig. 1).

(Fig. 1 near here)

2.6. Statistical analysis

All quantitative results were expressed as the mean ± SD. The number of slices examined is given in parentheses. One-way analysis of variance with Scheffé's post hoc test was used to compare the data. Statistical significance was set at $p < 0.05$, unless otherwise indicated.

3. Results

Hippocampal CA1 pyramidal neurons with stable membrane potentials more negative than −60 mV were used for the following studies. The resting membrane potential and the apparent input resistance in CA1 neurons were −74.1 ± 1.6 mV (n = 161) and 38 ± 10 MΩ (n = 161), respectively. The slice preparations were pretreated with drugs and exposed to ischemia only once.

3.1. Effects of cathepsin L inhibitors on the irreversible depolarization induced by OGD

We examined the involvement of cathepsin L in the membrane potential changes produced by OGD in hippocampal CA1 pyramidal neurons. Slice preparations were treated with potent and cell-permeable inhibitors of cathepsin L, cathepsin L inhibitors I and IV. Treatment with the cathepsin L inhibitors at all concentrations tested induced weak and inconsistent potential changes—hyperpolarization or depolarization of a few millivolts—before OGD, but no significant differences were observed in the resting membrane potential (data not shown). Figs. 2A and 3A show the typical potential changes in CA1 neurons during and after OGD in the absence (control) and presence of cathepsin L inhibitor I (2 nM) or cathepsin L inhibitor IV (20 nM). Under control conditions, OGD

induced a sequence of potential changes consisting of an initial hyperpolarization, a slow depolarization, and then a rapid depolarization (Figs. 2A and 3A, top). When oxygen and glucose were reintroduced immediately after the rapid depolarization, the membrane depolarized further (persistent depolarization), reaching 0 mV within 5 min. Thereafter, the membrane never recovered to the potential before exposure to OGD (irreversible depolarization). The amplitude and the duration of the initial hyperpolarization under control conditions were −5.1 ± 2.9 mV and 2.8 ± 0.8 min (n = 51), respectively. The latency and the maximal slope of the rapid depolarization in the control were 4.8 ± 0.7 min and 8.2 ± 3.2 mV/s (n = 51), respectively.

When slices were pretreated with cathepsin L inhibitors I (2 nM) and IV (20 nM), the amplitudes of the initial hyperpolarization were significantly different from the control (−8.2 ± 3.2 mV (n = 14) and −8.3 ± 1.2 mV (n = 10), respectively). In contrast, the durations of the initial hyperpolarization were not significantly different (2.9 ± 0.7 min (n = 14) and 3.6 ± 0.6 min (n = 10), respectively). The latency and the maximal slope of the rapid depolarization also did not significantly differ from control (4.2 ± 0.6 min and 6.9 ± 3.5 mV/s (n = 14), 4.9 ± 0.8 min and 8.6 ± 2.0 mV/s (n = 10), respectively). These results indicate that neither cathepsin L inhibitor affects the rapid depolarization.

(Figs. 2 and 3 near here)

Each of the cathepsin L inhibitors partially restored the membrane potential to the pre-exposure level after the reintroduction of oxygen and glucose following the rapid depolarization (Figs. 2A, B and 3A, B). The percentage of neurons exhibiting recovery from the irreversible depolarization induced by OGD was dependent on the concentration of the cathepsin L inhibitor (Figs. 2B and 3B). The effects of the cathepsin L inhibitors on the membrane potential 30 min after the reintroduction of oxygen and glucose (30 min post-OGD) are shown in Figs. 2C and 3C. In the absence of cathepsin L inhibitors (control condition), the membrane potential 30 min post-OGD was −3.4 ± 4.4 mV (n = 51). With treatment with cathepsin L inhibitor I, the membrane potential 30 min post-OGD repolarized toward pre-exposure levels in a concentration-dependent manner, as follows: 300 pM, −15.9 ± 20.0 mV (n = 10, not significant); 500 pM, −13.8 ± 24.7 mV (n = 10, not significant); 1 nM, −35.3 ± 26.9 mV (n = 14, $p < 0.01$); 1.5 nM, −44.0 ± 21.4 mV (n = 9, $p < 0.01$); 2 nM, −53.9 ± 28.2 mV (n = 14, $p < 0.01$). With treatment with cathepsin L inhibitor IV, the membrane potential 30 min post-OGD significantly repolarized toward pre-exposure levels in a

concentration-dependent manner, as follows: 300 pM, −9.1 ± 16.8 mV (n = 9, not significant); 1 nM, −17.4 ± 16.3 mV (n = 9, $p < 0.05$); 2 nM, −20.3 ± 19.1 mV (n = 10, $p < 0.05$); 10 nM, −36.8 ± 14.0 mV (n = 9, $p < 0.01$); 20 nM, −42.6 ± 18.8 mV (n = 10, $p < 0.01$); 30 nM, −49.5 ± 27.4 mV (n = 8, $p < 0.01$).

To clarify whether the repolarization of membrane potential produced by cathepsin L inhibitors 30 min post-OGD is mediated by the inhibition of cathepsin L activity, the relative recovery ratio (%Recovery) was calculated, and the concentration dependency of the %Recovery was analyzed for cathepsin L inhibitor IV, which is a selective and reversible reagent. The %Recovery effectuated by cathepsin L inhibitor IV increased in a concentration-dependent manner (Fig. 4A). When the %Recovery values were fitted to the Michaelis–Menten equation using a nonlinear regression analysis program (Kaleida Graph Version 4.01) (shown as a solid curve in Fig. 4A), the 50% effective concentration of cathepsin L inhibitor IV was 1.81 nM. These results suggest that cathepsin L contributes to the generation of the irreversible depolarization induced by OGD.

3.2. Morphological changes in the presence of cathepsin L inhibitors 30 min post-OGD

We next examined the morphological features of biocytin-labeled neurons after OGD in the absence and presence of the cathepsin L inhibitors since the membrane dysfunction was followed by the morphological damage in most CA1 neurons tested. Under control conditions, the cell body became swollen, and the proximal apical dendrite eventually fragmented into pieces in recorded CA1 neurons (Fig. 4B, b). In contrast, in recorded CA1 neurons treated with the cathepsin L inhibitors, the cell body and proximal apical dendrite appeared normal, and the cells exhibited a complete restoration of membrane potential, similar to control neurons not subjected to OGD (Fig. 4B, a and c). The long and transverse axes of control neurons not subjected to OGD were, respectively, 34.0 ± 9.4 μm and 19.3 ± 3.0 μm (n = 9). The long and transverse axes of neurons treated with cathepsin L inhibitor IV were, respectively, 34.0 ± 3.9 μm and 18.6 ± 2.8 μm (n = 7, not significant).

(Fig. 4 near here)

4. Discussion

In hippocampal CA1 neurons, cathepsin L inhibitors significantly restored the membrane potential after OGD to pre-exposure levels in the majority of neurons tested, and they yielded the recovery from the persistent depolarization after OGD. These results suggest that cathepsin L contributes to the generation of the irreversible depolarization.

4.1. Effects of cathepsin L inhibitors on the electrophysiological and morphological changes induced by OGD

Cathepsin L inhibitors, such as I and IV, provide protection against the persistent depolarization and the ensuing irreversible depolarization elicited by OGD. Cathepsin L inhibitor I is a potent, cell-permeable, selective and *irreversible* inhibitor of cathepsin L. Cathepsin L inhibitor I at 1–2 nM significantly restored the membrane potential 30 min post-OGD to pre-exposure levels. This concentration is similar to that shown to inhibit neuronal death induced by quinolinic acid in rat striatal neurons [18]. Cathepsin L inhibitor IV is a potent, cell-permeable, selective and *reversible* inhibitor of cathepsin L. Cathepsin L inhibitor IV at 1–30 nM significantly restored the membrane potential 30 min post-OGD to pre-exposure levels. The %Recovery provided by cathepsin L inhibitor IV increased in a

253 concentration-dependent manner. When the membrane potential 30 min post-OGD recovered
254 to the pre-exposure level, 100% inhibition of membrane dysfunction was considered to have
255 been achieved by cathepsin L inhibitor IV. The 50% effective concentration of cathepsin L
256 inhibitor IV would therefore provide a %Recovery of 50%. The 50% effective concentration
257 (1.81 nM) was similar to the IC_{50} for cathepsin L (1.9 nM), determined using recombinant
258 human cathepsin L purified from mouse myeloma cells [19]. Therefore, the concentration of
259 cathepsin L inhibitor IV used in this study was high enough to inhibit cathepsin L. In the
260 presence of the cathepsin L inhibitors, the rapid depolarization induced by OGD was not
261 affected, and biocytin-labeled neurons did not become swollen nor did they exhibit
262 membrane dysfunction 30 min post-OGD. It is therefore possible that cathepsin L inhibitors
263 affect the persistent depolarization, thereby preventing the establishment of irreversible
264 depolarization. These results suggest that the activation of cathepsin L is an important event
265 in the irreversible membrane dysfunction induced by OGD.

266 In slices pretreated with the cathepsin L inhibitor, there was a significant increase in the
267 amplitude of the initial hyperpolarization. Because the hyperpolarization in rat hippocampal
268 CA1 neurons is mainly caused by the activation of ATP-sensitive potassium channels by the
269 reduction in $[ATP]_i$ following hypoxia [2], our findings suggest that cathepsin L inhibitors

affect the ATP-sensitive potassium conductance. However, further studies are required to clarify the mechanisms underlying the increase in the initial hyperpolarization.

4.2. Mechanisms underlying the irreversible depolarization induced by OGD

In general, OGD induces an accumulation of extracellular glutamate (Glu), which activates ionotropic Glu receptors (NMDA and/or AMPA/kainate-type receptors). The activation of ionotropic Glu receptors produces a depolarization that increases Ca^{2+} influx through NMDA and voltage-gated Ca^{2+} channels. The influx of Ca^{2+} also induces Ca^{2+}-activated Ca^{2+} release from intracellular Ca^{2+} stores (e.g., endoplasmic reticulum) [3]. These processes increase the intracellular Ca^{2+} concentration ($[Ca^{2+}]_i$) further. The accumulated extracellular Glu activates the metabotropic Glu receptor, which in turn activates phospholipase C (PLC). The activated PLC produces diacylglycerol (DAG) and inositol triphosphate (IP_3) from membrane phospholipids. IP_3 increases the $[Ca^{2+}]_i$ further by enhancing release of Ca^{2+} from intracellular Ca^{2+} stores. The resulting high $[Ca^{2+}]_i$ triggers the activation of phospholipase A2 (PLA_2), adenylate cyclase (via Ca^{2+}/calmodulin) and nitric oxide (NO) synthase to produce arachidonic acid, cAMP and NO, respectively. DAG

activates protein kinase C (PKC), and cAMP activates protein kinase A (PKA). PKC and PKA enhance NMDA and AMPA/kainate Glu receptors [20-25]. Furthermore, activated PKA augments the activity of nitric oxide synthase (NOS) [11,26]. Cytochrome P-450 metabolizes arachidonic acid, resulting in the production of oxygen radicals [27,28]. NO reacts with oxygen radicals to yield peroxynitrite ($ONOO^-$) [11]. $ONOO^-$ and/or oxygen radicals damage the cytoskeleton and induce peroxidation of membrane lipids, which likely contributes to the large blebs and cell swelling observed in rat CA1 pyramidal neurons during the persistent depolarization [12].

In the present study, the cathepsin L inhibitors significantly restored the membrane potential 30 min post-OGD toward the pre-exposure level, similar to the effects of free radical and NO scavengers in our previous studies [11,12]. The treatment with the cathepsin L inhibitors prevented the morphological changes, including swelling of the cell body and fragmentation of dendrites, observed in the control neurons after OGD. Oxygen radicals induce lysosomal membrane permeabilization and trigger the release of cathepsins from lysosomes after OGD [13]. Therefore, it is possible that $ONOO^-$ and/or oxygen radicals induce lysosomal membrane permeabilization and the release of cathepsin L, which in turn causes the irreversible depolarization (Fig. 5).

(Fig. 5 near here)

Acknowledgments

This work was partly supported by a Grant-in-Aid for Scientific Research (C) from the Japan Society for the Promotion of Science, and by the Ministry of Education, Culture, Sports, Science and Technology by establishing open research centers in private universities.

References

[1] E. Tanaka, S. Yamamoto, Y. Kudo, S. Mihara, H. Higashi, Mechanisms underlying the rapid depolarization produced by deprivation of oxygen and glucose in rat hippocampal CA1 neurons in vitro, J Neurophysiol. 78 (1997) 891–902.

[2] N. Fujimura, E. Tanaka, S. Yamamoto, M. Shigemori, H. Higashi, Contribution of ATP-sensitive potassium channels to hypoxic hyperpolarization in rat hippocampal CA1 neurons in vitro, J Neurophysiol. 77 (1997) 378–385.

[3] S. Yamamoto, E. Tanaka, Y. Shoji, Y. Kudo, H. Inokuchi, H. Higashi, Factors that reverse the persistent depolarization produced by deprivation of oxygen and glucose in rat hippocampal CA1 neurons in vitro, J Neurophysiol. 78 (1997) 903–911.

[4] E. Tanaka, S. Yamamoto, H. Inokuchi, T. Isagai, H. Higashi, Membrane dysfunction induced by in vitro ischemia in rat hippocampal CA1 pyramidal neurons, J Neurophysiol. 81 (1999) 1872–1880.

[5] H.A. Kontos, Oxygen radicals in cerebral vascular injury, Circ Res. 57 (1985) 508–516.

[6] B.K. Siesjö, C.D. Agardh, F. Bengtsson, Free radicals and brain damage, Cerebrovasc Brain Metab Rev. 1 (1989) 165–211.

329 [7] P.H. Chan, Role of oxidants in ischemic brain damage, Stroke. 27 (1996) 1124–1129.

330 [8] H.A. Kontos, Oxygen radicals in cerebral ischemia: the 2001 Willis lecture, Stroke. 32
331 (2001) 2712–2716.

332 [9] M.V. Avshalumov, M.E. Rice, NMDA receptor activation mediates hydrogen
333 peroxide-induced pathophysiology in rat hippocampal slices, J Neurophysiol. 87 (2002)
334 2896–2903.

335 [10] T. Hayashi, A. Saito, S. Okuno, M. Ferrand-Drake, R.L. Dodd, T. Nishi, C.M. Maier, H.
336 Kinouchi, P.H. Chan, Oxidative damage to the endoplasmic reticulum is implicated in
337 ischemic neuronal cell death, J Cereb Blood Flow Metab. 23 (2003) 1117–1128.

338 [11] M. Onitsuka, S. Mihara, S. Yamamoto, M. Shigemori, H. Higashi, Nitric oxide
339 contributes to irreversible membrane dysfunction caused by experimental ischemia in rat
340 hippocampal CA1 neurons, Neurosci Res. 30 (1998) 7–12.

341 [12] E. Tanaka, S. Niiyama, S. Sato, A. Yamada, H. Higashi, Arachidonic acid metabolites
342 contribute to the irreversible depolarization induced by in vitro ischemia, J Neurophysiol.
343 90 (2003) 2113–3223.

[13] J.A. Windelborn, P. Lipton, Lysosomal release of cathepsins causes ischemic damage in the rat hippocampal slice and depends on NMDA-mediated calcium influx, arachidonic acid metabolism, and free radical production, J Neurochem. 106 (2008) 56–69.

[14] R. Durmaz, H. Özden, G. Kanbak, E. Aral, O.C. Arslan, K. Kartkaya, K. Uzuner, The protective effect of dexanabinol (HU-211) on nitric oxide and cysteine protease-mediated neuronal death in focal cerebral ischemia, Neurochem Res. 33 (2008) 1683–1691.

[15] T. Yamashima, S. Oikawa, The role of lysosomal rupture in neuronal death, Prog Neurobiol. 89 (2009) 343–358.

[16] Y. Kohda, T. Yamashima, K. Sakuda, J. Yamashima, T. Ueno, E. Kominami, T. Yoshioka, Dynamic Changes of Cathepsins B and L Expression in the Monkey Hippocampus after Transient Ischemia, Biochem Biophys Res Commun. 228 (1996) 616-622.

[17] T. Yamashima, Y. Kohda, K. Tsuchiya, T. Ueno, J. Yamachima, T. Yoshioka, E. Kominami, Inhibition of ischemic hippocampal neuronal death in primates with cathepsin B inhibitor CA-074: a novel strategy for neuroprotection based on 'calpain-cathepsin hypothesis', Eur J Neurosci. 10 (1998) 1723-1733.

[18] Y.R. Wang, S. Qin, R. Han, J.C. Wu, Z.Q. Liang, Z.H. Qin, Y. Wang, Cathepsin L plays a role in quinolinic acid-induced NF-Kb activation and excitotoxicity in rat striatal neurons, PLoS One. 8 (2013) e75702.

[19] T. Yasuma, S. Oi, N. Choh, T. Nomura, N. Furuyama, A. Nishimura, Y. Fujisawa, T. Sohda, Synthesis of peptide aldehyde derivatives as selective inhibitors of human cathepsin L and their inhibitory effect on bone resorption, J Med Chem. 41 (1998) 4301–4308.

[20] L.Y. Wang, M.W. Salter, J.F. MacDonald, Regulation of kainate receptors by cAMP-dependent protein kinase and phosphatases, Science. 253 (1991) 1132–1135.

[21] L. Aniksztejı, S. Otani, Y. Ben-Ari, Quisqualate metabotropic receptors modulate NMDA currents and facilitate induction of long-term potentiation through protein kinase C, Eur J Neurosci. 4 (1992) 500–505.

[22] B.U. Keller, M. Hollmann, S. Heinemann, A. Konnerth, Calcium influx through subunits GluR1/GluR3 of kainate/AMPA receptor channels is regulated by cAMP dependent protein kinase, EMBO J. 11 (1992) 891–896.

375 [23] R. Cerne, K.I. Rusin, M. Randic, Enhancement of the N-methyl-D-aspartate response in
376 spinal dorsal horn neurons by cAMP-dependent protein kinase, Neurosci Lett. 161
377 (1993) 124–128.
378 [24] W.Y. Lu, Z.G. Xiong, S. Lei, B.A. Orser, E. Dudek, M.D. Browning, J.F. MacDonald,
379 G-protein-coupled receptors act via protein kinase C and Src to regulate NMDA
380 receptors, Nat Neurosci. 2 (1999) 331–338.
381 [25] V.A. Skeberdis, V. Chevaleyre, C.G. Lau, J.H. Goldberg, D.L. Pettit, S.O. Suadicani, Y.
382 Lin, M.V.L. Bennett, R. Yuste, P.E. Castillo, R.S. Zukin, Protein kinase A regulates
383 calcium permeability of NMDA receptors, Nat Neurosci. 9 (2006) 501–510.
384 [26] Y. Xu, T.L. Krukoff, Adrenomedullin stimulates nitric oxide production from primary rat
385 hypothalamic neurons: roles of calcium and phosphatases, Mol Pharmacol. 72 (2007)
386 112–120.
387 [27] M.S. Paller, H.S. Jacob, Cytochrome P-450 mediates tissue-damaging hydroxyl radical
388 formation during reoxygenation of the kidney, Proc Natl Acad Sci USA. 91 (1994)
389 7002–7006.
390 [28] B.K. Siesjö, K. Katsura, Ischemic brain damage: focus on lipids and lipid mediators, In:
391 Neurobiology of Essential Fatty Acids, Adv Exp Med Biol. 318 (1992) 41–56.

392 **Figure captions**

393

394 Fig. 1. Protocol for the calculation of the relative recovery ratio (%Recovery). The horizontal
395 white bar indicates treatment with the cathepsin L inhibitors. The horizontal gray bar
396 indicates the period of oxygen and glucose deprivation (OGD). The upper most dotted line
397 indicates 0 mV potential. The membrane potential 30 min post-OGD (b) divided by the
398 resting membrane potential (a) yields the %Recovery.

399

400 Fig. 2. Effects of cathepsin L inhibitor Ⅰ on membrane potential changes produced by
401 OGD in rat hippocampal CA1 neurons. (A) Typical changes in membrane potential during
402 and after OGD in the absence of an inhibitor (control, top trace) and in the presence of
403 cathepsin L inhibitor I (bottom trace). OGD was conducted between the period indicated by
404 the downward and upward arrows. The dotted lines in each trace show the pre-exposure
405 membrane potential (−74 and −75 mV from top to bottom). Downward deflections show
406 hyperpolarizing potentials elicited by anodal current pulses (0.2–0.4 nA, 200 ms duration, 3s
407 intervals). In the presence of cathepsin L inhibitor I, the membrane potential recovered to the
408 resting membrane potential after re-perfusion of oxygen and glucose. (B) Effect of cathepsin

409 L inhibitor I on the percentage of neurons exhibiting recovery from the irreversible
410 depolarization produced by OGD. Open columns, shaded columns and closed columns
411 indicate no, partial and complete recovery, respectively. (C) Effect of cathepsin L inhibitor I
412 on the membrane potential 30 min after re-perfusion of oxygen and glucose (30 min
413 post-OGD). In the presence of cathepsin L inhibitor I, the membrane potential repolarized
414 toward pre-ischemic levels in a concentration-dependent manner after re-perfusion of oxygen
415 and glucose. Each column shows mean ± SD. $^{**}p < 0.01$ (one-way analysis of variance with
416 Scheffé's post hoc test).
417
418 Fig. 3. Effects of cathepsin L inhibitor IV on membrane potential changes produced by OGD
419 in rat hippocampal CA1 neurons. (A) Typical changes in membrane potential during and after
420 OGD in the absence of an inhibitor (control, top trace) and in the presence of cathepsin L
421 inhibitor IV (bottom trace). The dotted lines in each trace show the pre-exposure membrane
422 potential (−74 and −73 mV from top to bottom). (B) Effect of cathepsin L inhibitor IV on the
423 percentage of neurons exhibiting recovery from the irreversible depolarization produced by
424 OGD. Open columns, shaded columns and closed columns indicate no, partial and complete
425 recovery, respectively. (C) Effect of cathepsin L inhibitor IV on the membrane potential 30

426 min after re-perfusion of oxygen and glucose (30 min post-OGD). In the presence of
427 cathepsin L inhibitor IV, the membrane potential repolarized toward pre-ischemic levels in a
428 concentration-dependent manner after re-perfusion of oxygen and glucose. Each column
429 shows mean ± SD. *$p < 0.05$, **$p < 0.01$ (one-way analysis of variance with Scheffé's post
430 hoc test).
431
432 Fig. 4. (A) Changes in the relative recovery ratio (%Recovery) following the administration
433 of cathepsin L inhibitor IV. %Recovery increases in a manner dependent on the concentration
434 of the cathepsin L inhibitor. Solid curve shows the %Recovery fitted with the Michaelis–
435 Menten equation using a nonlinear regression analysis program (Kaleida Graph Version 4.01).
436 (B) A biocytin-labeled pyramidal neuron after 30 min in normal Krebs solution (a). A
437 biocytin-labeled pyramidal neuron 30 min post-OGD in the absence of inhibitor (b). A
438 biocytin-labeled pyramidal neuron 30 min post-OGD in the presence of cathepsin L inhibitor
439 (c). △, soma. ▲, dendrite. Scale bar indicates 10 μm.
440
441 Fig. 5. Putative mechanisms contributing to the generation of the irreversible depolarization
442 induced by OGD. OGD induces the activation of several signaling mechanisms that increase

443 $[Ca^{2+}]_i$ and result in the irreversible depolarization. Lysosomal membrane permeabilization

444 (LMP) causes the release of cathepsins and other hydrolases from the lysosome into the

445 cytosol. Peroxynitrite ($ONOO^-$) and/or oxygen radicals induce LMP and the release of

446 cathepsin L, which in turn causes the irreversible depolarization.

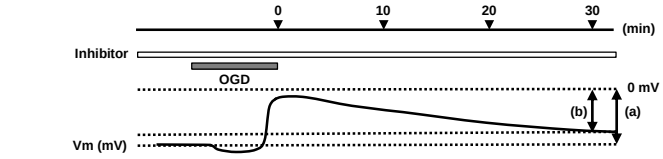

$$\% \text{ Recovery} = \frac{(b)}{(a)} \times 100\ (\%)$$

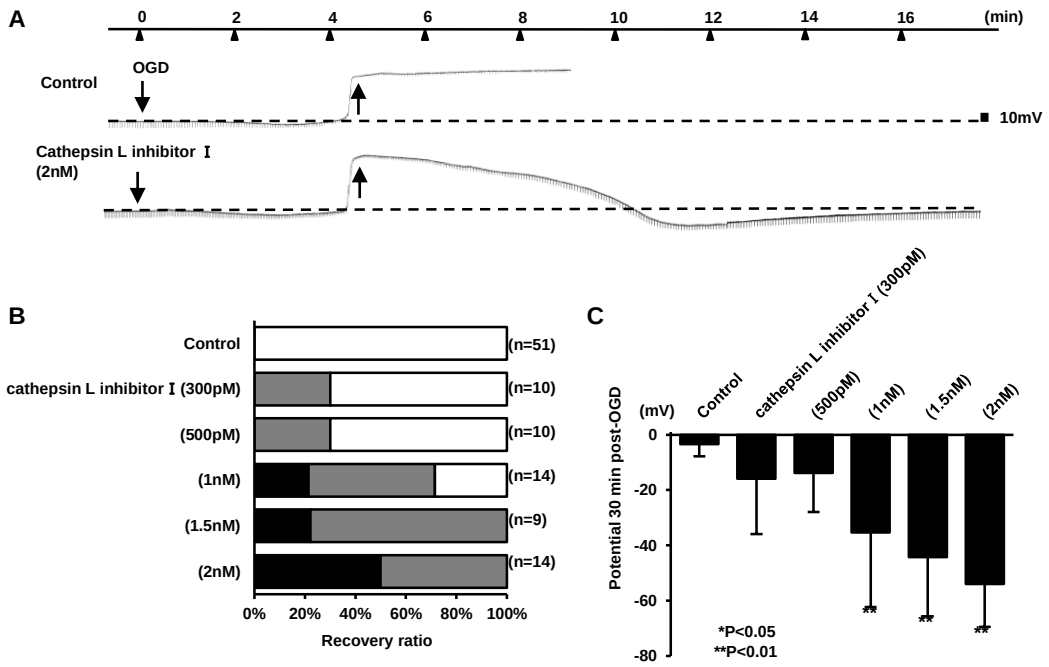
A
0
2
4
6
8
10
12
14
16
(min)
Control
OGD
10mV
Cathepsin L inhibitor Ⅰ
(2nM)
B
Control
cathepsin L inhibitor Ⅰ (300pM)
(500pM)
(1nM)
(1.5nM)
(2nM)
(n=51)
(n=10)
(n=10)
(n=14)
(n=9)
(n=14)
0%
20%
40%
60%
80%
100%
Recovery ratio
C
Cathepsin L inhibitor Ⅰ (300pM)
(mV)
Control
(500pM)
(1nM)
(1.5nM)
(2nM)
Potential 30 min post-OGD
0
-20
-40
-60
-80
*P<0.05
**P<0.01

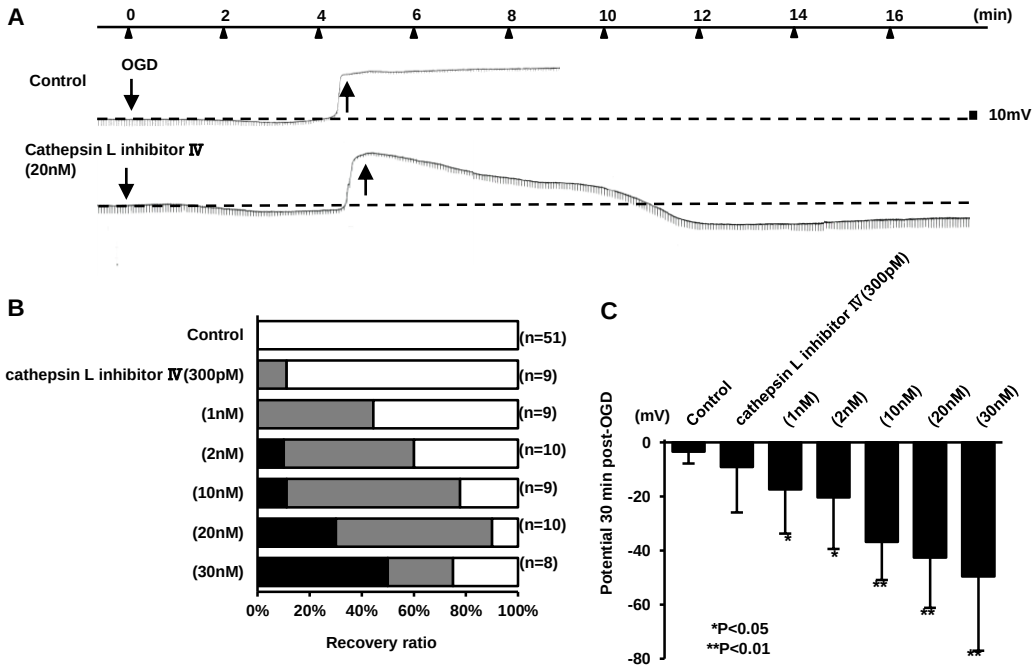
A
0
2
4
6
8
10
12
14
16
(min)
Control
OGD
10mV
Cathepsin L inhibitor Ⅳ
(20nM)
B
Control
cathepsin L inhibitor Ⅳ(300pM)
(1nM)
(2nM)
(10nM)
(20nM)
(30nM)
(n=51)
(n=9)
(n=9)
(n=10)
(n=9)
(n=10)
(n=8)
0%
20%
40%
60%
80%
100%
Recovery ratio
C
cathepsin L inhibitor Ⅳ(300pM)
(mV)
Control
(1nM)
(2nM)
(10nM)
(20nM)
(30nM)
Potential 30 min post-OGD
0
-20
-40
-60
-80
*P<0.05
**P<0.01

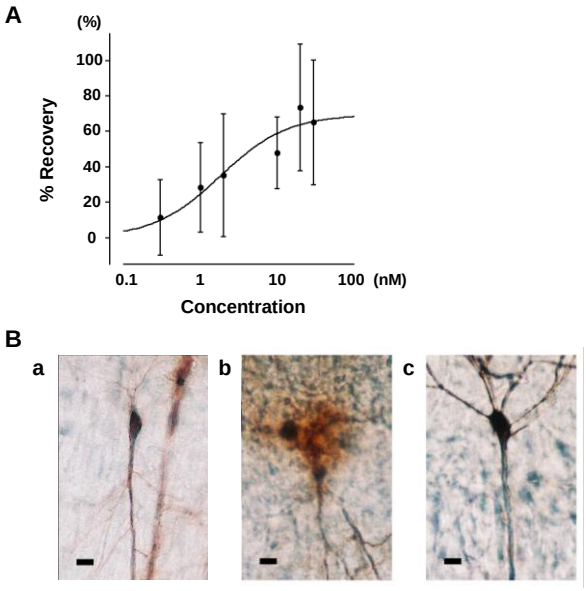
A
(%)
100
80
60
40
20
0
% Recovery
0.1
1
10
100
(nM)
Concentration
B
a
b
c

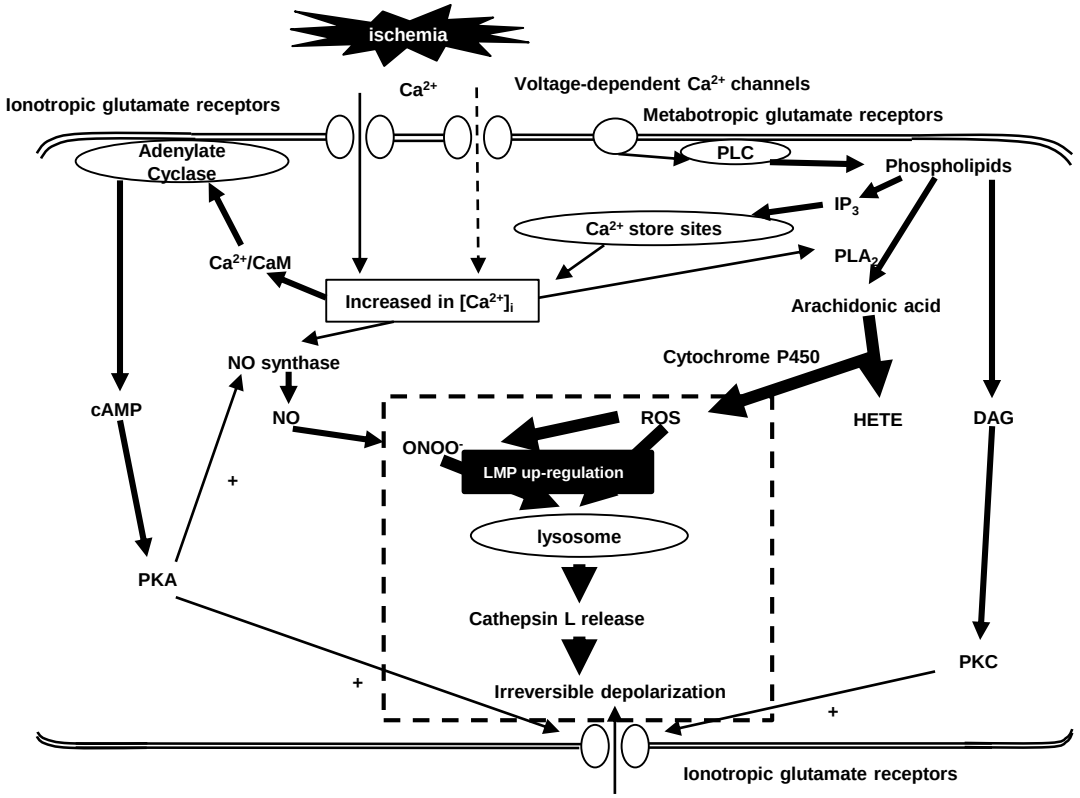
ischemia
Ca2+
Voltage-dependent Ca2+ channels
Ionotropic glutamate receptors
Metabotropic glutamate receptors
Adenylate Cyclase
PLC
Phospholipids
IP3
Ca2+ store sites
Ca2+/CaM
PLA2
Increased in [Ca2+]i
Arachidonic acid
NO synthase
Cytochrome P450
cAMP
NO
ROS
HETE
DAG
ONOO-
LMP up-regulation
+
lysosome
PKA
Cathepsin L release
PKC
+
Irreversible depolarization
+
Ionotropic glutamate receptors